

International Conference on Space Optics—ICSO 2022

Dubrovnik, Croatia

3–7 October 2022

Edited by Kyriaki Minoglou, Nikos Karafolas, and Bruno Cugny,



High-Power Free-Space Bulk Multiplexer for Satellite Communication Optical Ground Terminal



High-Power Free-Space Bulk Multiplexer for Satellite Communication Optical Ground Terminal

Fabrizio Silvestri^a, Linda W. Feenstra^b, Federico Pettazzi^a, Jan R. Nijenhuis^b, Jan de Vreugd^b, Dick de Bruijn^a, Remco den Breeje^b, Wimar A. Klop^b, and Ivan Ferrario^b

^aTNO Optics Department, Stieltjesweg 1, Delft, The Netherlands

^bTNO Optomechatronics Department, Stieltjesweg 1, Delft, The Netherlands

ABSTRACT

High throughput optical satellite communication (SATCOM) systems need to rely on effective and robust technology to enable wavelength-division multiplexing (WDM) in a commercially viable way. The main challenge to implement WDM in optical feeder links deals with the multiplexing of high power channels. Currently the levels of power required for communication, tens of watts per channel, make unfeasible to multiplex several channels in a waveguiding device. A free space architecture is devised to mitigate this issue. The paper describes the architectural choices made, the optical and mechanical design for a multiplexer to be employed in a Optical Feeder Link terminal combining 13 channels, each carrying 50 W of optical power. Within the TOmCAT (Terabit Optical communiCation Adaptive Terminal) project a demonstrator of the full system has been realized. The demonstrator multiplexer supports 5 channels, each carrying up to 2 W of optical power, with an optical bandwidth of 25 GHz, centered on the 200 GHz ITU grid. The design and the experimental results obtained during the integration of the multiplexer demonstrator are here presented and discussed.

Keywords: Optical Satellite Communication, High Power Beam Combining, Multiplexer, Diffraction Grating

1. INTRODUCTION

The research of optical satellite communication is growing enormously in the last decades. Amongst the different areas of investigation, the technology development around optical feeder links (OFLs) represents one of the key challenge. OFLs are thought to be able to feed GEO-stationary satellites with data modulated on optical carriers. Owing to their intrinsic larger absolute bandwidth, and the more confined spatial distribution of optical beams, less prone to being intercepted, optical communication system promises to complement current Radio Frequency (RF) satellite communication (SATCOM) systems. Especially, the large bandwidth offers the possibility to reach high data rate with optical systems in the range of Terabit per second (Tbit/s).

Within TOmCAT TNO has investigated the technology development for optical feeder links which can reach Tbit/s communication data rate, with help of adaptive optics pre-correction on the uplink beam.^{1,2}

One key ingredient for reaching the Tbit/s throughput is the capability to implement Wavelength Division Multiplexing (WDM) paradigms in an OFL architecture. WDM enables the combination of different data channels on the same free space optical link. The main challenge in implementing a WDM architecture in an optical ground terminal (OGT) is represented by the optical power levels of the beams to be combined. The optical power carried by each beam should be in the order of tens of watts, to close an optical link with a GEO-stationary satellite from ground.¹ Typical optical multiplexer implemented in fiber or waveguided technology cannot cope with such power levels, and therefore a possible solution to this challenge is to resort to a free space multiplexing.

Free space beam combination is a relatively established approach to reach high optical power levels, in the order of kW, in a single optical beam. Typically, the beam combination is achieved by means of optical components which exhibit different propagation paths as function of the spectral beam characteristics, for example diffraction gratings^{3,4} or dichroic filters.⁵ The use of diffraction gratings has shown to be advantageous with respect to dichroic filters, since the latter may suffer from thermomechanical modifications of the coatings under continuous

Further author information: (Send correspondence to F.S.)
F.S.: E-mail: fabrizio.silvestri@tno.nl

exposure of high irradiance beams. While established for applications related to high energy lasers (HEL), the use of spectral beam combination (SBC) in the field of optical communication is relatively novel. Both applications require a highly efficient transfer of optical power via a free space path, however, satellite optical communication adds an additional level of complexity, because any SBC architecture should be as minimally invasive as possible on the transmitted data quality. Moreover, SBC requires typically a series of optical free space components (gratings, filters, mirrors) which need to be kept mechanically stable over time to ensure the tighter requirements on pointing stability of SATCOM system compared to typical HEL applications. The use of diffraction gratings for SBC in a WDM optical SATCOM architecture is foreseen also in other works,⁶ where two identical gratings are coupled to combine the optical beams. The coupled-grating solution compensates for the angular dispersion characteristic of the grating which can deteriorate the data transmission on each channel. Rather than resorting on a coupled-grating concept, which could be complex to manage in view of the accurate alignment needed between the two gratings, in this paper the use of a single grating to implement SBC for an OFL is presented. The design of the Bulk Multiplexer (BMUX) is based on several system considerations, involving communication, optical and mechanical aspects. The principles followed to design the TOMCAT BMUX are discussed in detail in a previous work.⁷

The paper is organized as follows: in section 2 the system requirements for the TOMCAT OFL system are introduced with the scope of deriving the subsystem requirements for the BMUX; in section 3 the BMUX architecture of the demonstrator is described, together with a detailed discussion of the optical and mechanical design, breadboard and integration tests results; finally, the discussion of the results achieved and the conclusions on the work are reported in section 4.

2. TOMCAT OPTICAL FEEDER LINK BULK MULTIPLEXER

2.1 Optical Feeder Link System Requirements

The TOMCAT project is meant to develop commercially viable optical ground stations to enable laser links for Very High Throughput Satellites carrying laser communication payloads. The final goal is to develop technology able to reach 1 Tbit/s communication throughput. One key feature of the TOMCAT architecture is the use of adaptive optics (AO) for the downlink, but also for the pre-correction of the uplink beam. A system diagram of the TOMCAT OFL is reported in Figure 1. A set requirements for the OFL are reported in Table 1. The requirements reported are limited to those one relevant for the design of the BMUX subsystem. With 13 uplink channels, and 7 downlink channels, each of 100 Gbit/s, the TOMCAT OFL is sized to support a gross throughput of ≥ 2 Tbit/s.

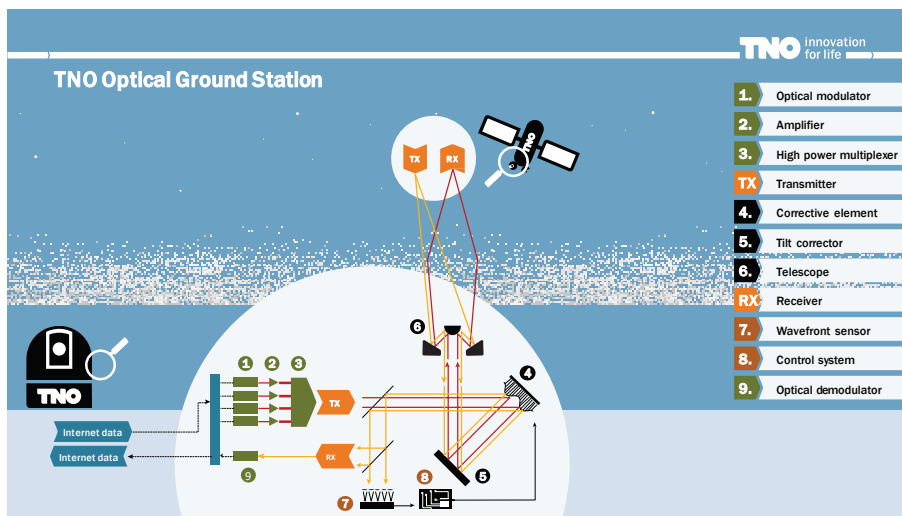


Figure 1: System diagram of TOMCAT OFL employing AO.

Table 1: TOMCAT OFL Requirements.

Uplink Bandwidth	1535 – 1555 nm
Uplink Number of Channels	13
Uplink Optical Power per Channel	50 W
On-sky Uplink Beam Half-Angle ($1/e^2$) Divergence	$5.3 \mu\text{rad}$
Downlink Bandwidth	1565 – 1578 nm
Downlink Number of Channels	7
OGT Telescope Aperture Diameter	600 mm
OGT Telescope Relative Linear Obscuration	23%
Magnification OGT Telescope	$\times 6$
Magnification OGT AO Bench	$\times 9.8$
Channel Spacing	200 GHz / 1.6 nm
Single channel datarate	100 Gbit/s
Modulation Format	QPSK

2.2 Grating Dispersion Effects on Communication

The angular dispersion of a grating in a BMUX introduces a filtering process on the communication signal spectrum.⁷ The effect of the angular dispersion can be compensated by the use of a coupled-gratings.⁶ However, in this case any clipping aperture in the OGT optical layout could induce wavelength-dependent losses, since the signal content is spatially spread over the apertures of the OGT. This effect is dual to the spatial spreading at receiver side in case of use of a single grating. For the TOMCAT OFL the choice is to have a single grating and it is justified by reduced complexity in alignment and stability of a single combining component. The effect of the frequency filtering can be modeled in analytical terms as a frequency-dependent normalized insertion loss⁷

$$IL(f) = e^{-2 \frac{[(f-f_0)c_0 D]^2}{(f_0^2 M \theta_0)^2}}, \quad (1)$$

where f_0 is the carrier frequency of the modulated signal, c_0 the speed of light, M the magnification of the optical system following the grating, θ_0 the half-angle divergence of the beam on-sky, and $D = 1/(\Lambda \cos \alpha_{in})$ is the grating angular dispersion, which is dependent on the grating period, Λ , and the angle of incidence of the beams on the grating, α_{in} . From equation 1 it is clear that the angular dispersion should be minimized to contain the filtering fall-off. On the other side the angular dispersion, together with the channel spacing, dictates the angular spacing between the different channels beams, and consequently the total volume of the system. The decision for the TOMCAT BMUX is to go for a combination of spatial and spectral multiplexing.⁷ By fitting two uplink beams in the same OGT it is possible to distribute the channels over two independent gratings, each of them combining only a subset of the total channels. The advantage is that the effective channel spacing on the single grating can be increased by a factor 2, when the channels are distributed in an alternated way on the two gratings. It is important to note that in this case the two gratings are independent, and their orientation does not need to be coupled as in the coupled-gratings scenario.⁶

To understand better the effect of frequency filtering on the communication signal, a test with a satellite emulator setup was built during the design phase. The breadboard, shown in Figure 2, is meant to emulate in the lab the signal propagation of a real optical link to a GEO-stationary satellite. The OGT side is constituted by a bit pattern generator, Sympuls BP32G, which feeds a Pseudo-Random Bit Stream into a transceiver, iXBlue ModBox NRZ-series. The modulated optical signal is coupled to free space via a collimator, Thorlabs AL2550J-C, and sent to a transmission grating, Ibsen Photonics PING-600-045-ds. The optical beam exiting the grating is sent via a fine steering mirror, Optics in Motion OIM101, to the receiver end of the link, consisting of a focusing lens, Thorlabs AL2550J-C, and a receiving fiber. The received signal is processed by an oscilloscope, Tektronix

DPO70000SX, to generate bit stream statistics. To extract the effect of the grating on the communication, a set of three folding mirrors are introduced in the optical path, effectively by-passing the grating. By running bit-stream statistics with this by-pass in place, a reference case for the comparison between propagation with and without grating effect is established. Bit-Error-Ratio (BER) analyses have been run different levels of received power. For this purpose the transmitter optical power has been calibrated in the two configuration, to have the same level of received optical power at the receiving fiber.

The two identical lenses of the transmitter and receiver side have been size to be representative of the TOmCAT OFL link. According to the specifications of Table 1, assuming a square waveform for the baseband signal, the first zero of the baseband signal is 50 GHz apart from the carrier. With a typical angular dispersion in the order of $700 \mu\text{rad}$, equation 1 results in a relative penalty at the edge of the bandwidth of about -7.0 dB . Due to hardware limitations, the breadboard could only support On-Off Key (OOK) modulation, with a maximum analog bandwidth of 25 GHz. At the fiber receiver, the combination of two lenses with $f = 50 \text{ mm}$ leads to an overlapping integral for the fiber coupling which is characterized by a Gaussian shape with a penalty of about -7.0 dB at 25 GHz. In this way the equivalence between the experimental setup and TOmCAT link is established.

The curves of BER vs received power, shown in Figure 2, indicates that the presence of the grating introduces a penalty of additional 3.0 dB in the minimum received power threshold, needed to achieve $BER = 10^{-4}$. It is important to note that this penalty arises from a pure optical power loss, as integral effect of the product of the filter transfer function and baseband signal spectrum, and an additional loss due to the low-pass nature of the effective filter implemented by the angular dispersion.

The breadboard results show the presence of a penalty when the BMUX is implemented with angular dispersion element like a grating. Nevertheless, this loss can be accounted in the overall link budget of the system, in view of possible advantages from the side of the opto-mechanical design.

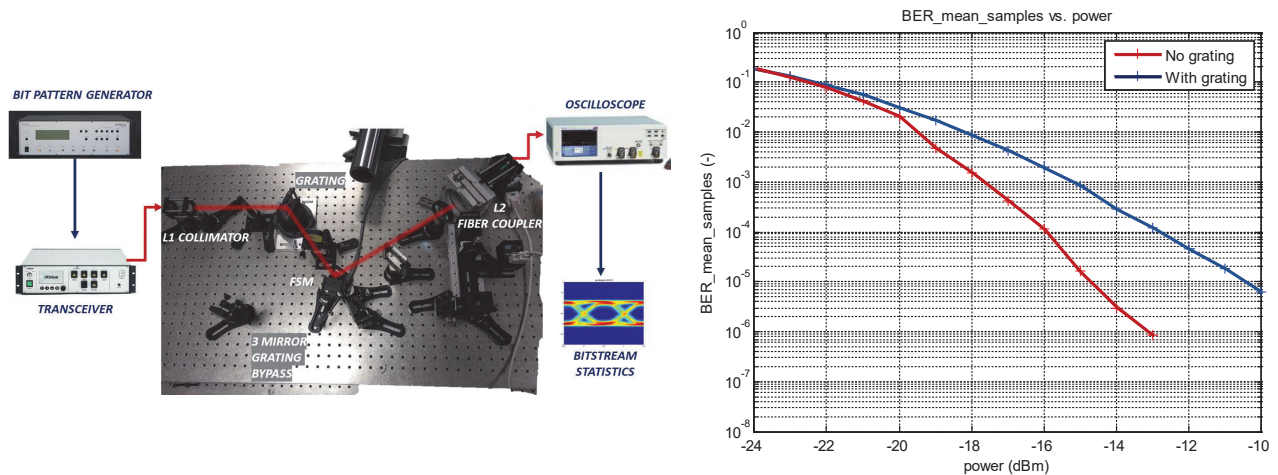


Figure 2: Satellite Emulator Breadboard (left) and BER vs Received Power experimental results (right).

2.3 TOmCAT BMUX Requirements

Based on the TOmCAT OFL requirements, Table 1, and the knowledge of the effect of the angular dispersion, section 2.2, it is possible to derive paraxial requirements for the optical layout the BMUX. The resulting requirements are summarized in Table 2. The proposed optical layout handling the selected requirements is reported in Figure 3. It includes a duplication of the optical path to implement a spatial multiplexing of the transmitter with two beams. The optical path is folded by two folding mirrors, FM1-FM3 and FM2-FM4, respectively, and the group of optical beams are incident on two independent gratings, G1 and G2. A roof-top mirror, RTM, is envisioned to combined the two subset of multiplexed beams before interfacing with the rest of the OFL.

Table 2: TOmCAT BMUX derived requirements

Spatial Multiplexing Channel Spacing Factor	2
Effective Signal Bandwidth	40 GHz
Grating Angular Dispersion	700 $\mu\text{rad}/\text{nm}$
Grating Line Period	600 mm^{-1}
Relative Insertion Loss at Edge Bandwidth	-4.7 dB
Collimator Half-Angle ($1/e^2$) Divergence	270 μrad
Collimator Minimum Lateral Dimension	12 mm

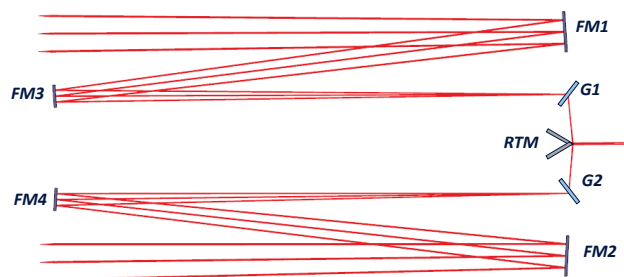


Figure 3: BMUX Optical Layout

In Table 2 with the parameter effective spectral separation is meant the spectral separation between two adjacent beams in a single grating, which is two times the channel separation, owing to the spatial multiplexing. Moreover, the effective signal bandwidth is only 80% of the nominal 50 GHz, since some low-pass filtering is implemented in electrical domain of the system.

The collimator half-angle divergence is just derived from the combined magnification of the OGT telescope and OGT AO bench, since the BMUX is followed by these optical systems. Moreover, to avoid additional diffraction losses, due to angular dispersion, it is required that each optical beam incident on the grating is characterized by a relatively flat wavefront. This is achieved by requiring that the real waist of the optical beam is located in the neighborhood of the grating surface.

The collimator is a critical component which requires a careful design. On top of the optical performance, the collimator should satisfy challenging functional and environmental requirements, such accurate alignment capability (tip-tilt alignment resolution $< 10, \mu\text{rad}$), reduced form factor ($< 10 \text{ mm}$ lateral footprint) and it should be able to withstand high level of optical power ($\geq 50 \text{ W}$ per single channel). The focal length of the collimator can be derived by balancing concurrent requirements: the beam divergence, the position of the waist on the grating, and the minimum lateral dimension of the collimator. For the latter, the requirement reported in Table 2 comes from several discussion with optics manufacturers. The optimal focal length for the collimator is found to be 27 mm. By placing the fiber termination in a defocused position, it is possible to achieve a beam with the waist at about 6.3m from the collimator aperture, and with the required divergence.⁸ The need for such long working distance arises from the minimum lateral spacing between adjacent channels and the grating angular dispersion.

3. BULK MULTIPLEXER DEMONSTRATOR: DESIGN, INTEGRATION AND TESTS

Within the TOmCAT project, a demonstrator of the full chain of an OFL has been designed, integrated and tested.⁹ The aim of the demonstrator is to show the feasibility of technologies to achieve $> 1 \text{ Tbit/s}$ optical communication. The demonstrator includes an OGT demonstrator and a Satellite Terminal Breadboard (STB), separated by 10km on a ground-to-ground optical link. A demonstrator of the BMUX is also realized and integrated in the OGT demonstrator. The BMUX demonstrator differs from the BMUX design discussed in section 2.3, since it needs to adapt to the different requirements of the OGT demonstrator.

3.1 Subsystem Requirements

The requirements of the BMUX Demonstrator are reported in Table 3. These requirements have been derived to adapt to the OGT demonstrator, which is downgraded with respect to the original TOmCAT system design in terms of optical power level, number of channels and overall throughput. Nevertheless, the philosophy behind the demonstrator is to build a system which is as representative as possible to the original design. From this perspective it can be seen that the angular dispersion filtering is matched to the demonstrator signal bandwidth,

Table 3: TOMCAT BMUX Demonstrator requirements

Uplink Bandwidth	1535 – 1555 nm
Uplink Number of Channels	5
Uplink Optical Power per Channel	2 W
Uplink Datarate	25 Gbit/s
Uplink Modulation Format	OOK
Effective Signal Bandwidth	20 GHz
Grating Angular Dispersion	700 $\mu\text{rad}/\text{nm}$
Grating Line Period	600 mm^{-1}
OGT Magnification	$\times 10$
On-sky Uplink Beam Half-Angle ($1/e^2$) Divergence	16 μrad
Relative Insertion Loss at Edge Bandwidth	-4.3 dB
Collimator Half-Angle ($1/e^2$) Divergence	270 μrad
Collimator Minimum Lateral Dimension	12 mm
Collimator-Sky Magnification	$\times 18$

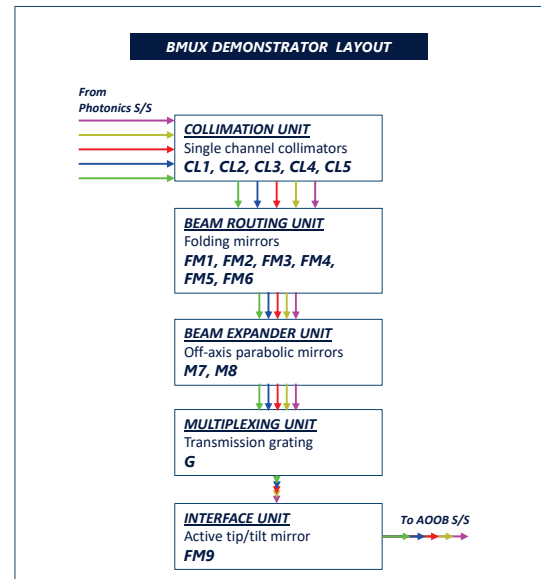


Figure 4: BMUX Demonstrator Subsystem Layout. Components labels refer to optical design layout of Figure 5

as the BMUX demonstrator imposes the same penalty as in the original design Table 2. Moreover, the collimator is also characterized by the same specifications as in the original design. In this way, the optomechanical properties of the collimator, and its mounting adjusters, can be verified during the test campaign. To match the collimator divergence to the magnification of the OGT demonstrator, and to the final uplink beam divergence, compared to the initial design, a different architecture is used. This is visualized in the system layout of Figure 4. After the collimators and folding mirrors used to fold the path, a beam expander with a magnification of $\times 1.8$ is introduced. The role of this expansion is two-fold: on one side it reduces the beam divergence to be close to the required on-sky divergence of 16 μrad , on the other side it increases the angular spacing between the beam, as seen from the grating. In addition to the beam expander just mentioned, an additional tip-tilt actively controlled mirror is introduced, to facilitate the alignment of the multiplexed beams towards the OGT AO bench. With the goal of representativeness of the BMUX demonstrator as key subsystem for a future OFL, it is also required in the selection of components that the BMUX system should be compatible to cope also with high level of optical power, as the final product should be able to support > 350 W of aggregated optical power. This leads to the preference in the design for reflective optics, where possible, and for transmissive components which can cope with the high optical power levels.

3.2 Optical Design

A 3D render of the demonstrator optical design is reported in Figure 5 with the list of components used and specifications in Table 4. For each single beam the optical path involves the following components: a collimator (CL) which re-images the fiber waist at about 6.3 m from the aperture, a series of folding mirrors FM1 to FM6, which helps to keep the BMUX footprint within an area of 1800 mm \times 935 mm. The crossing point of all beams is located at the beam waist location. Moreover, this is also the location of the entrance pupil of a beam expander (BEX) composed by a pair of off-axis parabolic mirrors, M7 and M8, which implements a magnification of $\times 1.8$. A transmission grating (G) is located at the exit pupil plane of the BEX. All the five beams are incident at an angle on the diffraction close enough to the Littrow angle of the grating, to ensure high diffraction efficiency, but with an angular margin of a couple of degrees to avoid that the reflected first order of diffraction of the grating



Figure 5: 3D render of the optical design of the BMUX demonstrator.

Table 4: BMUX Demonstrator Optical Components.

CL1,...,CL5	Fiber Collimator, $f = 27$ mm, clear aperture diameter 8 mm
FM1,...,FM6	Precision Optical Protected Silver coated Fused Silica folding mirrors, clear aperture $156 \text{ mm} \times 32 \text{ mm}$, reflectivity $> 98\%$
M7	Off-axis parabolic mirror, Radius of Curvature 400 mm, clear aperture diameter 36 mm, decenter 30 mm
M8	Off-axis parabolic mirror, Radius of Curvature 720 mm, clear aperture diameter 36 mm, decenter 54 mm
G	Ibsen Photonics PING-600-045ds, Fused Silica Transmission Grating, line frequency 600 mm^{-1} , clear aperture $40 \text{ mm} \times 40 \text{ mm}$, diffraction efficiency $> 90\%$
FM9	Edmund Optics #43-416-577, Protected Silver Fused Silica folding mirrors, clear aperture diameter 45.7 mm, reflectivity $> 98\%$

falls back on the collimators. Finally another folding mirror, FM9, folds the beam upwards where the interface with the OGT AO Optical Bench (AOOB) will be located.

According to the requirements, the magnification of the BEX, together with the OGT magnification, will reduce the beam divergence of a factor $\times 18$, reducing the initial collimator divergence to $15 \mu\text{rad}$. However, it must be highlighted that due to the mechanical constraints, the collimator aperture and the effective aperture of the OGT clip partially the uplink beam. The effect of this clipping has been numerically analyzed and it is calculated that the effective final divergence on-sky meets the requirement of $16 \mu\text{rad}$.

The five channels implemented in the BMUX are not uniformly distributed on the allocated spectral band,

and therefore they are also not uniformly distributed spatially. The channels wavelength of each beam and their relative angular position are reported in Table 5.

Table 5: BMUX Demonstrator Channel Wavelengths and Angle of Arrival at BEX Entrance Pupil.

Channel Number	Wavelength (nm)	Angle of Arrival (μrad)
1	1536.6	10.4
2	1545.3	0.0
3	1551.7	-7.7
4	1553.3	-9.6
5	1554.4	-11.5

3.3 Mechanical Design

The mechanical design has been focused on the critical components and aspects which can affect the stability performance of the full system. The beams at the output of the BMUX Demonstrator should exhibit a maximum angular misalignment with respect to the beams centroid of $< 20 \mu\text{rad}$ after alignment, and of $< 27 \mu\text{rad}$ over an interval of operation of 2 hours, including drift effects. The allocation of the several pointing error contributors lead to a situation in which the most stringent components require a stability of $< 5 \mu\text{rad}$ for tip and tilt: the mounting of the collimators determining the individual beam pointing, the mounting of the set of folding mirrors and the beam expander determining the optical quality of the beam wavefront.

In the BMUX demonstrator aluminium optical components, mounts and other parts are used where possible, leading to a more homogeneous temperature distribution throughout the system.

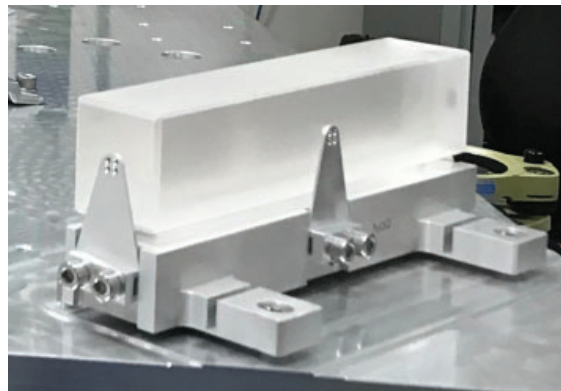


Figure 6: Folding mirror assembly

The five collimators are mounted into separate tip-tilt mounts. An aperture in the mount allows the beam to pass through the mechanism without sensible optical clipping losses. The lateral spacing of the collimators limits the footprint of the mount resulting in a highly compact monolithic flexure-based tip-tilt mechanism. The collimator can hinge around the horizontal axis by a double lever creating a virtual rotation line close to the collimator lens. The rotation around the vertical axis is created by a hinge in front of the collimator. The tip-tilt adjustments can be performed manually using a preloaded fine adjustment screw. By spacing the collimators longitudinally it is possible to take advantage of extra space for mounting the mechanisms and adjusting the tip-tilt mechanisms. A resolution of $< 10 \mu\text{rad}$ can be easily achieved with this manual adjustment for both tip and tilt. The required beam pointing stability due to mechanical drifts of the designed mount has been verified experimentally. The tests involved in this verification are described in section 3.4.

The six identical flat folding mirrors are each held by an identical mount, shown in Figure 6. This mount is composed of a base structure with three out-of-plane leaf springs attached to it. The leaf springs define a thermal

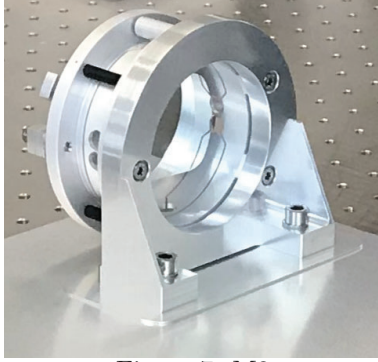


Figure 7: M8



Figure 8: Grating assembly

center in the middle of the folding mirror body and cope with the difference in thermal expansion coefficient between the aluminum mount and fused silica mirror. The leaf springs are fixated to the mirrors with a spot of glue. The sixth mirror is adjusted with its entire mount in tip, by means of an additional pre-loaded alignment screw, and tilt to provide an adjustment for the spatial alignment of the beams incident on the grating.

The two off-axis parabolic mirrors, M7 and M8, are placed and aligned onto a separate base plate to form the beam expander assembly. A dedicated mount is manufactured to fixate M7 on the separate base plate. M8 is mounted to a flexure-based cardan hinge surrounding M8 with virtual rotation point in the center of the mirror, Figure 7. Manual actuation of preloaded alignment screws provides tip and tilt motion of M8 with respect to M7 with a resolution of $<10 \mu\text{rad}$, as required by the chosen alignment strategy.

The grating is mounted into a mount with a thin walled frame with a few droplets of glue. The frame is compliant enough to cope with the difference in thermal expansion coefficient between the aluminum mount and fused silica grating.

3.4 Breadboard Tests

A breadboard test was conducted to study the pointing stability of the optical beam exiting from each collimator. According to the requirements of Table 3, the test has been conducted with up to 2 W of optical power carried by a single beam.

The beam pointing of the collimator is measured by a pointing assembly composed of a Newport KPX633 lens ($f=884 \text{ mm}$) with a Dataray BR2-IGA slit camera mounted at the focal plane. The angular position of the beam with respect of the lens optical axis can be tracked by this system over time. The pointing assembly has been commissioned in the laboratory and a measurement accuracy of $<3 \mu\text{rad}$ has been achieved considering all the error contributors. This is in line with the range of pointing variation that are needed to be tracked by the tool. The beam pointing after the collimator is required to be stable within $<5 \mu\text{rad}$ over 2 hours of operation at laboratory temperature conditions. Each measurement run consists of 2 hours of pointing observations over the two axis, 1. Each datapoint is obtained by averaging 10 s of raw measurements acquired at 2 Hz.

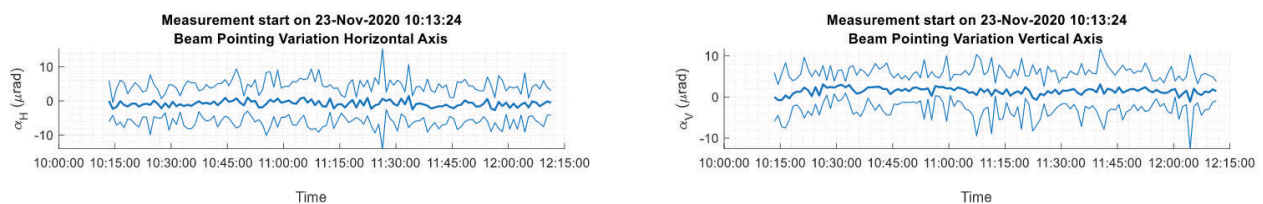


Figure 9: Beam pointing measurement of the collimator in its prototype mount over 2 hours at 2 W. Thick solid line: mean value for each measurement point, thin solid line $3 - \sigma$ variation range for each measurement point.

Figure 9 shows the horizontal and vertical beam pointing position with respect to the initial measurement measured over 2 hours. It is observed that no remarkable drift behaviour is seen for the beam pointing position.

Assuming a statistical confidence of 3 standard deviation, it is observed that the pointing of the beam can be characterized to be stable within $\pm 5 \mu\text{rad}$, in agreement with the requirements. The test results confirm the design strategy for the collimator mount.

It is important to highlight that breadboard activities on pointing stability were limited to the collimator adjusters/mounts, because these are the main contributors of pointing errors at individual channel level. This type of error is more critical than the common channel error which arises from components like the folding mirrors, BEX and grating. To compensate for this common error the use of the active tip tilt adjustment of FM9 is foreseen.

3.5 System Integration and Test Results

The BMUX demonstrator has been built and integrated in the TOMCAT OGT demonstrator. More details about the full OGT demonstrator and the results of the test campaign can be found in another paper from the same group.⁹ Pictures from the final integrated BMUX demonstrator and of the full OGT containing the BMUX demonstrator are shown in Figure 10. Once the subsystem has been fully assembled, several tests have been conducted to verify the performance of the system.

The first test conducted was on the beam half-angle divergence of the multiplexed beam. The divergence of each beam has been measured at the output of the BMUX with the help of the same optical pointing assembly, as described in 3.4. All the beams show some ellipticity, as for channel 4, whose orthogonal profiles are reported in Figure 11. Nevertheless, the geometric average of the two axes divergence is compatible with the requirement of having $16 \mu\text{rad}$ half-angle divergence on the uplink beam. The measured half-angle divergences for the 5 channels are reported in Table 6 for two cases, with the camera axes parallel to the horizontal/vertical (H/V) direction and with them rotated of 45° (D).

Table 6: Half-angle divergence ($1/e^2$) for the 5 BMUX beams.

Channel Number	H/V Half-Angle Divergence (μrad)	D Half-Angle Divergence (μrad)
1	159.5	161.7
2	160.8	162.8
3	161.3	162.1
4	162.4	164.7
5	158.6	158.9

A second test was performed to verify the proper angular alignment of the 5 multiplexed beams and their stability over time. The requirement for proper multiplexing is that all beams point in the same direction. Moreover, in order to guarantee a stable communication, the pointing direction of each beam should be stable over time. Using the same optical setup used to measure the beam divergence, the relative angular inter-alignment of the beams have been measured after the initial alignment and re-sampled after 40 hours from the initial measurement. From the link budget a maximum inter-alignment error between the beams of $27.0 \mu\text{rad}$ was allocated for the BMUX. This error is defined output plane as a polar angle. In Figure 12 the results of the two measurement show that the initial inter-alignment of the beams is well within the requirement, with a maximum radial error of $3.0 \mu\text{rad}$. Moreover, after 40 hours, the setup exhibited only a global drift of maximum $20.0 \mu\text{rad}$. This does not represent a problem because global errors can be corrected with the tip-tilt mirror FM9, in between different measurement operations. Nevertheless, on the basis of these results it is advised for future commercial solutions to complement the transmitter subsystem, inclusive of the BMUX, with a real time pointing detector, to be able to lively compensate for this global drift during operation.

Finally, a test on the complete multiplexing performance was conducted. Pairs of different channels have been excited simultaneously. The multiplexed beam, containing the pair of beams excited, was coupled to a fiber with a lens (Thorlabs F280APC-1550, $f = 18.8 \text{mm}$). The fiber output was connected to an Optical Spectrum Analyzer (Yokogawa AQ6370), and the spectrum of the multiplexed beam was measured. The results of this

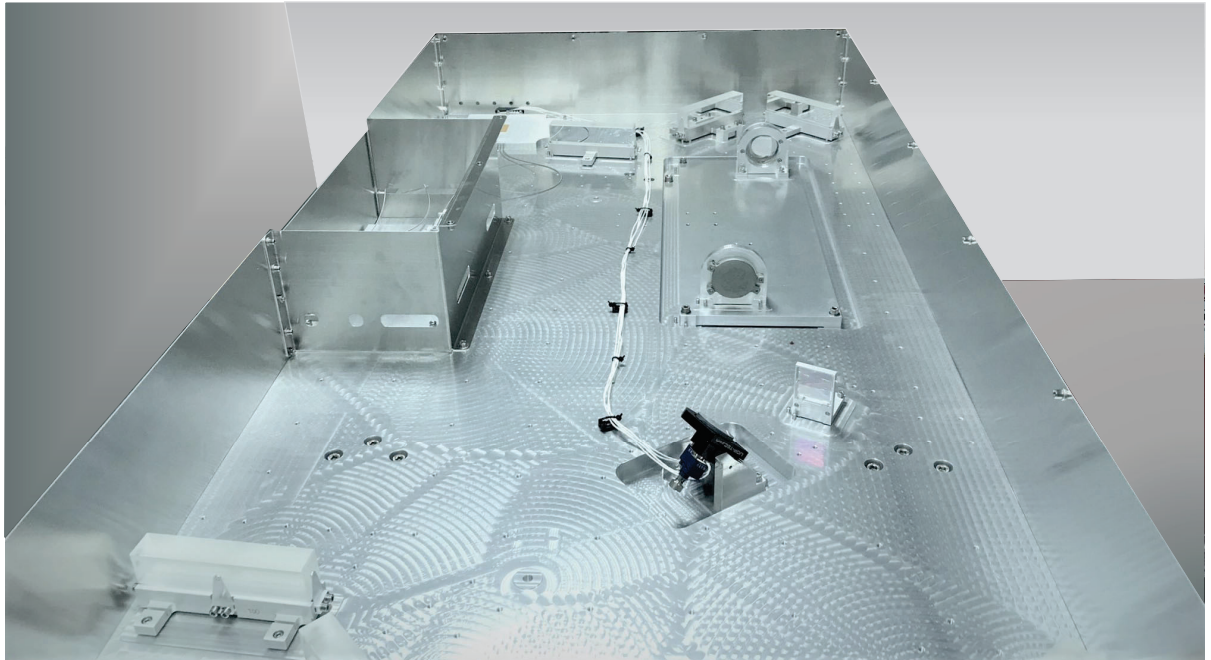


Figure 10: Pictures of TOmCAT BMUX and OGT demonstrators: the full BMUX demonstrator assembled (top); the OGT fully integrated with the BMUX below the main baseplate, covered by aluminium shields (bottom left); complete OGT transported to the test location for the ground-to-ground tests (bottom right).

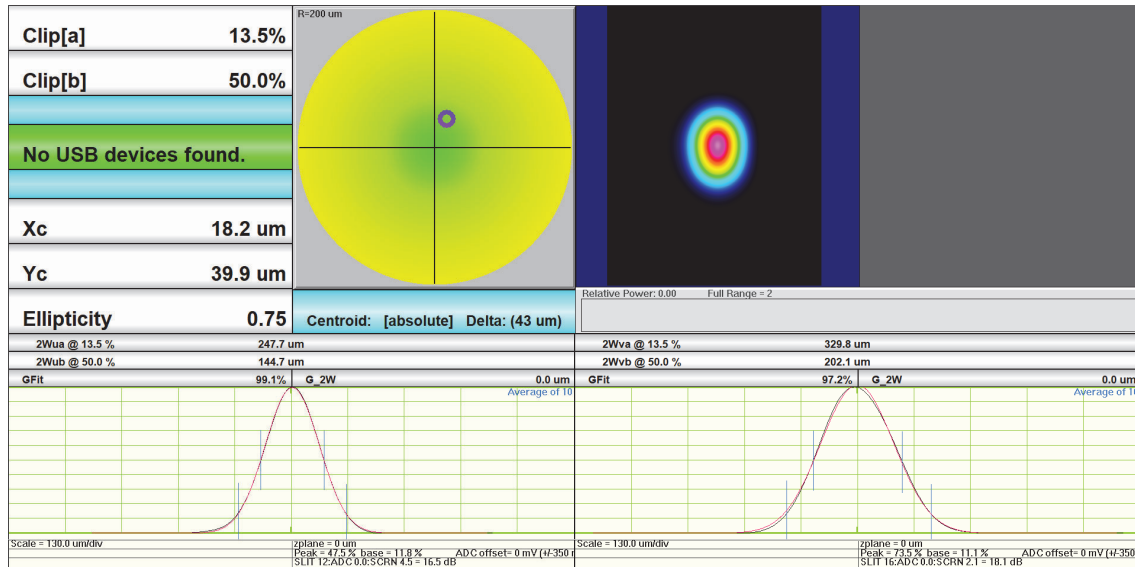


Figure 11: Irradiance profiles (horizontal, vertical) of channel 4 beam at the output of the BMUX, when focused with a lens $f = 887$ mm.

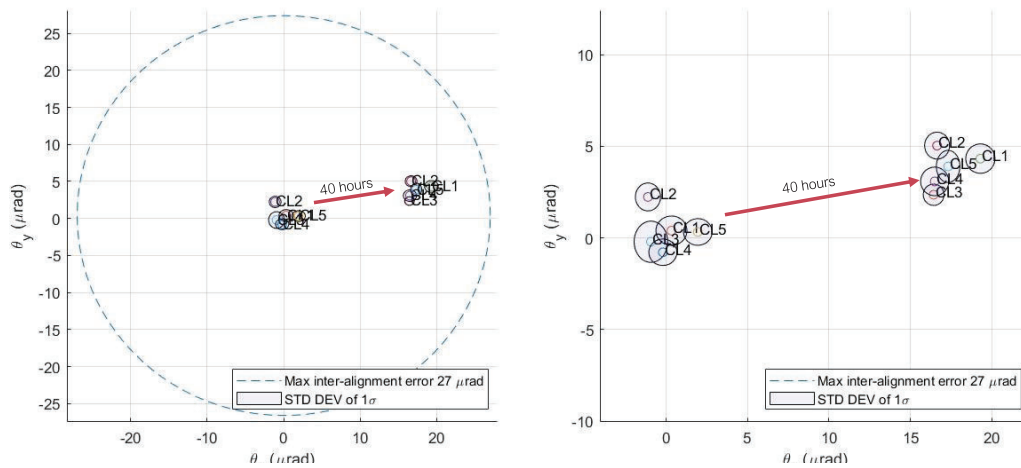


Figure 12: Angular centroid of 5 beams at the output beam. On the right a zoomed version of the picture on the left to show the relative low inter-alignment error and reduced global drift.

test are reported in Figure 13, with the full comb of 5 lines obtained as superposition of single measurements of pairs of beams. The measurements show that the relative power of each channel contained in the multiplexed beam is contained between variations of ± 1 dB, confirming the proper working of the system.

4. CONCLUSIONS

In this paper the BMUX of the TOMCAT optical feeder link is presented. The design strategy followed in agreement with the TOMCAT OFL system design has been described, with focus on the effect that a single grating based BMUX could have in the proper reception of the modulated signal. Experimental breadboard tests support the model proposed to account for this effect.

The demonstration activities developed within the TOMCAT project related the BMUX have been also described. The optical and mechanical designs of the system are discussed, with emphasis on the key-enabler of the BMUX.

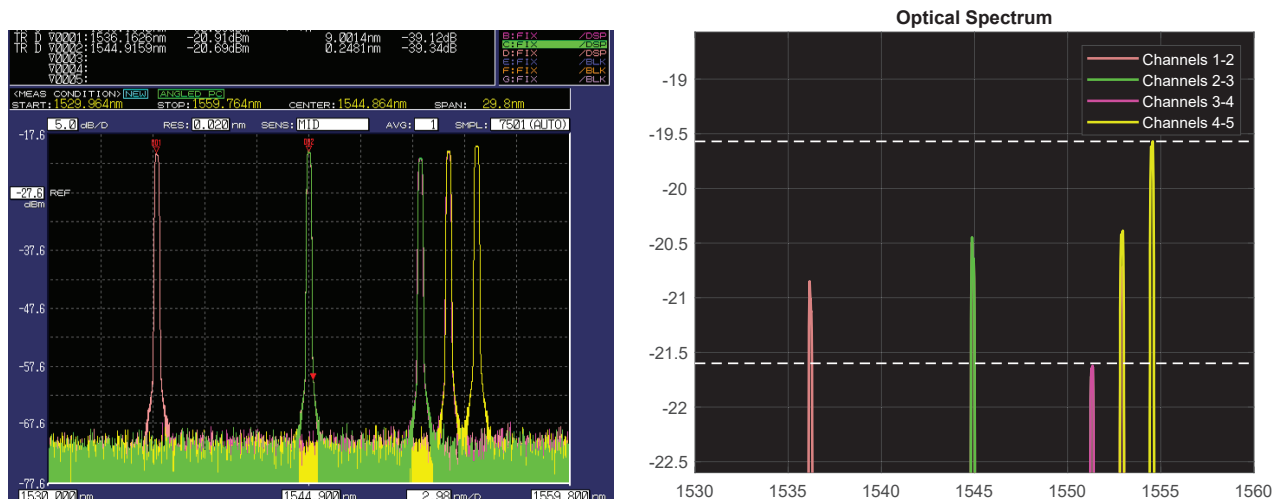


Figure 13: Output spectrum of the multiplexed beams. Pairs of channels have been excited in separate experiments and the results are over-imposed in this plot for clarity (left). Zoomed version of left picture, showing the relative difference in the spectral power density of the channels.

Finally, the integrated system is presented together with highlights on the verification tests performed. The integrated BMUX meets the initial requirements, enabling the multiplexing of 5 beams, in C-band. The optical components have been selected and designed to cope with optical power up to 50 W for each beam, although testing activity has been limited to 2 W per beam, due to hardware availability. The BMUX performance shows a inter-beam alignment within $3.0 \mu\text{rad}$ and a maximum global drift of $20.0 \mu\text{rad}$ at the BMUX output plane. This is considered acceptable for the TOMCAT field tests to maintain a stable optical link. Furthermore, the proper functioning of the BMUX has been checked by exciting multiple channels at the same time and analyzing with a spectrum analyzer the spectral content of the multiplexed beam. The relative intensity variation amongst the 5 channels is contained within $\pm 1 \text{ dB}$.

The tests conducted show how the presented BMUX system could be successfully employed for future Optical Feeder Link for GEO-stationary satellite. In addition, the design principles here employed could be extended to scale the design to an increased number of channels and or to different allocated transmission bands.

ACKNOWLEDGMENTS

Part of the work presented in this paper has been funded via the European Space Agency ARTES 4.0 programme “TOMCAT - Terabit Optical Communication Adaptive Terminal”.

The authors would like to acknowledge Dr. Zoran Sodnik (ESA - ESTEC) for the useful discussion during the different phases of the project, and Kristian Buchwald (Ibsen Photonics, DK) for the insights over performance and characterization of transmission gratings. Moreover, the authors would like to acknowledge Hittech Multin BV (NL) for the constructive cooperation during the execution of the project.

The collimator presented in this work has been custom-designed for this project by Doric Lenses Inc. (CA) under contract from MPB Communications Inc. (CA), partner of the TOMCAT project.

REFERENCES

- [1] Saathof, R., den Breeje, R., Klop, W., Kuiper, S., Doelman, N., Pettazzi, F., Vosteen, A., Truyens, N., Crowcombe, W., Human, J., Ferrario, I., Calvo, R. M., Poliak, J., Barrios, R., Giggenbach, D., Fuchs, C., and Scalise, S., “Optical technologies for terabit/s-throughput feeder link,” in [2017 IEEE International Conference on Space Optical Systems and Applications (ICSOS)], 123–129 (2017).

- [2] Saathof, R., den Breeje, R., Klop, W., Kuiper, S., Doelman, N., Pettazzi, F., Vosteen, A., Wildschut, J., de Lange, D., Moens, T., Koster, S., Gruber, M., Spierdijk, H., Kerkhof, P., Russchenberg, T., Truyens, N., Crowcombe, W., Human, J., Calvo, R. M., Poliak, J., Barrios, R., Scalise, S., and Ferrario, I., “Optical feeder link program and first adaptive optics test results,” in [*Free-Space Laser Communication and Atmospheric Propagation XXX*], Hemmati, H. and Boroson, D. M., eds., **10524**, 87 – 94, International Society for Optics and Photonics, SPIE (2018).
- [3] Zheng, Y., Yang, Y., Wang, J., Hu, M., Liu, G., Zhao, X., Chen, X., Liu, K., Zhao, C., He, B., and Zhou, J., “10.8 kw spectral beam combination of eight all-fiber superfluorescent sources and their dispersion compensation,” *Opt. Express* **24**, 12063–12071 (May 2016).
- [4] Strecker, M., Plötner, M., Stutzki, F., Walbaum, T., Ehrhardt, S., Benkenstein, T., Zeitner, U., Schreiber, T., Eberhardt, R., Tünnermann, A., Stuhr, U., Jung, M., and Ludewigt, K., “Highly efficient dual-grating 3-channel spectral beam combining of narrow-linewidth monolithic cw Yb-doped fiber amplifiers up to 5.5 kW ,” in [*Fiber Lasers XVI: Technology and Systems*], Carter, A. L. and Dong, L., eds., **10897**, 53 – 58, International Society for Optics and Photonics, SPIE (2019).
- [5] Chen, F., Ma, J., Wei, C., Zhu, R., Zhou, W., Yuan, Q., Pan, S., Zhang, J., Wen, Y., and Dou, J., “10 kw-level spectral beam combination of two high power broad-linewidth fiber lasers by means of edge filters,” *Opt. Express* **25**, 32783–32791 (Dec 2017).
- [6] Kernek, A. L., Canuet, L., Maho, A., Sotom, M., Matter, D., Francou, L., Edmunds, J., Welch, M., Kehayas, E., Perlot, N., Krzyzek, M., Paraskevopoulos, A., Leuthold, J., Horst, Y., Bourderionnet, J., Brignon, A., Lallier, E., Billault, V., Leviandier, L., Conan, J.-M., Védrenne, N., Lim, C. B., Montmerle-Bonnefois, A., Petit, C., Stampoulidis, L., Fehrenz, M., and Lehnigk-Emden, T., “The H2020 VERTIGO project towards tbit/s optical feeder links,” in [*International Conference on Space Optics — ICSO 2020*], Cugny, B., Sodnik, Z., and Karafolas, N., eds., **11852**, 508 – 519, International Society for Optics and Photonics, SPIE (2021).
- [7] Silvestri, F., Pettazzi, F., Eschen, M., Boschma, J. J., Lutgerink, J. B., Kramer, G. F. I. J., Korevaar, W. C., den Breeje, R., Duque, C. M., and Doelman, N. J., “Beam multiplexing for satellite communication optical feeder links,” in [*Free-Space Laser Communications XXXII*], Hemmati, H. and Boroson, D. M., eds., **11272**, 245 – 253, International Society for Optics and Photonics, SPIE (2020).
- [8] Self, S. A., “Focusing of spherical gaussian beams,” *Appl. Opt.* **22**, 658–661 (Mar 1983).
- [9] Broekens, K., Klop, W., Moens, T., Eschen, M., do Amaral Castro, G., Silvestri, F., Oosterwijk, A., Visser, M., Doelman, N., Saathof, R., and Ferrario, I., “Adaptive Optics pre-correction Demonstrator for Terabit Optical Communication Links,” in [*International Conference on Space Optics — ICSO 2022*], International Society for Optics and Photonics, SPIE.